Página legal de la revista, incluído el ISSN y la lista de índices en la que está incluída (Scopus, entre ellos)

ACS Publications
Most Trusted. Most Cited. Most Read.

ACS Journals ▾ | ACS eBooks ▾ | C&EN Global Enterprise

I&EC research
Industrial & Engineering Chemistry Research

Search | Citation | Subject | Advanced Search

Enter search text / DOI — Anywhere ▾ — Search
◉ Ind. Eng. Chem. Res. ○ All Publications/Website

🏠 | Browse the Journal | Articles ASAP | Current Issue | Submission & Review | Open Access | About the Journal

About the Journal

Editor: Phillip Savage
Department Head and Walter L.
Robb Family Endowed Chair
Professor of Chemical
Engineering, Pennsylvania
State University
E-mail: savage-
office@iecr.acs.org

Print Edition ISSN: 0888-5885
Web Edition ISSN: 1520-5045

View Publication Information in Current Issue

2017 Impact Factor: 3.141
2017 Total Citations: 67,598

Indexed/Abstracted in: CAS, SCOPUS, EBSCOhost,
Thomson-Gale (Gale Group), Proquest, British
Library, Ovid, Web of Science, and SwetsWise
ACS Divisions: Industrial & Engineering Chemistry

Journal Scope

Industrial & Engineering Chemistry, with variations in title and format, has been published since 1909 by the American Chemical Society. *Industrial & Engineering Chemistry Research* is a weekly publication that reports industrial and academic research in the broad fields of applied chemistry and chemical engineering with special focus on fundamentals, processes, and products.

Papers may be based on work that is experimental or theoretical, mathematical or descriptive, chemical or physical. In addition to fundamental research (in such areas as thermodynamics, transport phenomena, chemical reaction kinetics and engineering, catalysis, separations, interfacial phenomena, and materials), papers may deal with process design and development (for example, synthesis and design methods, systems analysis, process control, schemes for data correlation, modeling and scale-up procedures, etc.) and product research and development involving chemical and engineering aspects (for example, catalysts, plastics, elastomers, fibers, adhesives, coatings, paper, membranes, lubricants, ceramics, aerosols, etc.).

Select Decade ▾
Select Volume ▾
Select Issue ▾
List of Issues — Go

Portada del volumen 56 (17)

Table of Contents

May 3, 2017
Volume 56, Issue 17
Pages 4887-5146

About the Cover:

Graphics used on this cover have been selected from the following highlighted papers: M. Yang and F. You, "Comparative Techno-Economic and Environmental Analysis of Ethylene and Propylene Manufacturing from Wet Shale Gas and Naphtha" (DOI: 10.1021/acs.iecr.7b00354); L. Peng et al., "Maximizing the Density of Active Groups in Porous Poly(ionic liquids) for Efficient Adsorptive Desulfurization" (DOI: 10.1021/acs.iecr.6b04873); and T. Kurniawan et al., "Conversion of Dimethyl Ether to Olefins over Nanosized Mordenite Fabricated by a Combined High-Energy Ball Milling with Recrystallization" (DOI: 10.1021/acs.iecr.6b04834)

In this issue:

Download Hi-Res Cover

índice del Volumen 56 (selección de captura de pantallas). Se marca en recuadro rojo la sección donde aparece el artículo

REVIEWS

Abstract

ACS ActiveView PDF
Hi-Res Print, Annotate, Reference QuickView

PDF[2243K]

PDF w/ Links[872K]

Full Text HTML

Add to ACS ChemWorx

ACS Editors' Choice

Figure 1 of 8

APPLIED CHEMISTRY

Abstract | Supporting Info

ACS ActiveView PDF
Hi-Res Print, Annotate, Reference QuickView

PDF[4530K]

PDF w/ Links[713K]

Full Text HTML

Add to ACS ChemWorx

Figure 1 of 11

KINETICS, CATALYSIS, AND REACTION ENGINEERING

Abstract | Supporting Info

ACS ActiveView PDF
Hi-Res Print, Annotate, Reference QuickView

PDF[3049K]

PDF w/ Links[530K]

Full Text HTML

Add to ACS ChemWorx

Figure 1 of 10

Abstract

ACS ActiveView PDF
Hi-Res Print, Annotate, Reference QuickView

PDF[2621K]

PDF w/ Links[527K]

Full Text HTML

Add to ACS ChemWorx

Kinetic Investigation of the Solvent-Free Hydrogenation of Dehydroisophytol

Sergio Vernuccio, Adrian Meier, and Philipp Rudolf von Rohr
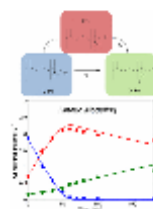
Figure 1 of 9

Abstract | Supporting Info

ACS ActiveView PDF
Hi-Res Print, Annotate, Reference QuickView

PDF[892K]

PDF w/ Links[492K]

Full Text HTML

Add to ACS ChemWorx

Branched 1,6-Diaminohexane-Derived Aliphatic Polyamine as Curing Agent for Epoxy: Isothermal Cure, Network Structure, and Mechanical Properties

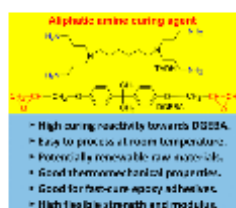Jintao Wan, Cheng Li, Hong Fan, and Bo-Geng Li

Figure 1 of 12

Abstract

ACS ActiveView PDF
Hi-Res Print, Annotate, Reference QuickView

PDF[2080K]

PDF w/ Links[685K]

Full Text HTML

Add to ACS ChemWorx

Visible-Light-Induced Atom-Transfer-Radical Polymerization with a ppm-Level Iron Catalyst

Chao Bian, Yin-Ning Zhou, Jun-Kang Guo, and Zheng-Hong Luo

Figure 1 of 8

Abstract

ACS ActiveView PDF
Hi-Res Print, Annotate, Reference QuickView

PDF[2257K]

PDF w/ Links[534K]

Full Text HTML

Add to ACS ChemWorx

MATERIALS AND INTERFACES

Experimental Study of the Effects of Using Different Precursor Concentrations, Solvent Types, and Injection Types on Solution Precursor High-Velocity Oxygen Fuel (HVOF) Nanostructured Coating Formation

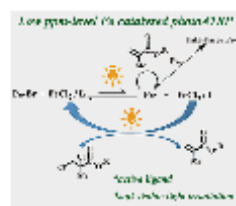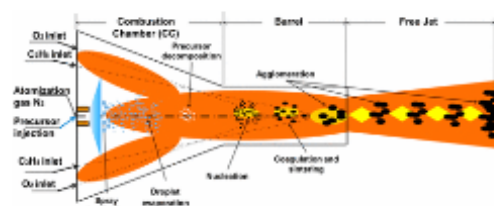Mahrukh Mahrukh, Arvind Kumar, and Sai Gu

Figure 1 of 13

Abstract

ACS ActiveView PDF
Hi-Res Print, Annotate, Reference QuickView

PDF[2246K]

PDF w/ Links[797K]

Full Text HTML

Add to ACS ChemWorx

Figure 1 of 20

THERMODYNAMICS, TRANSPORT, AND FLUID MECHANICS

☐ **Optimization of Detailed Schedule for a Multiproduct Pipeline Using a Simulated Annealing Algorithm and Heuristic Rules**
Haihong Chen, Changchun Wu, Lili Zuo, Feng Diao, Li Wang, Dapeng Wang, and Baoqiang Song
pp 5092-5106
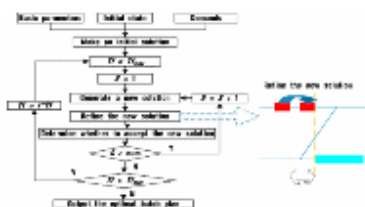**Publication Date (Web):** April 13, 2017 (Article)
DOI: 10.1021/acs.iecr.6b04745

Abstract

ACS ActiveView PDF
Hi-Res Print, Annotate, Reference QuickView

PDF[3443K]

PDF w/ Links[853K]

Full Text HTML

Add to ACS ChemWorx

Figure 1 of 23

☐ **Calculation of the Solubility Parameter by COSMO-RS Methods and Its Influence on Asphaltene–Ionic Liquid Interactions**
R. Hernández-Bravo, A. D. Miranda, O. Martínez-Mora, Z. Domínguez, J. M. Martínez-Magadán, R. García-Chávez, and J. M. Domínguez-Esquivel
pp 5107-5115
Publication Date (Web): April 17, 2017 (Article)
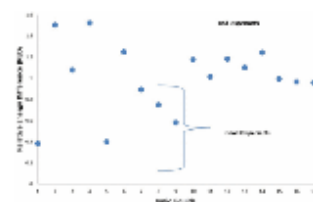**DOI:** 10.1021/acs.iecr.6b05035

Abstract | Supporting Info

ACS ActiveView PDF
Hi-Res Print, Annotate, Reference QuickView

PDF[2068K]

PDF w/ Links[469K]

Full Text HTML

Add to ACS ChemWorx

Figure 1 of 11

GENERAL RESEARCH

☐ **Split, Partial Oxidation and Mixed Absorption: A Novel Process for Synergistic Removal of Multiple Pollutants from Simulated Flue Gas**
Ping Fang, Zijun Tang, Xiongbo Chen, Jianhang Huang, Dingsheng Chen, Zhixiong Tang, and Chaoping Cen
pp 5116-5126
Publication Date (Web): April 3, 2017 (Article)
DOI: 10.1021/acs.iecr.6b05029
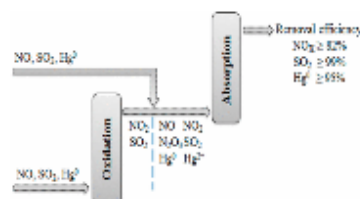
Abstract

ACS ActiveView PDF
Hi-Res Print, Annotate, Reference QuickView

PDF[2564K]

PDF w/ Links[617K]

Full Text HTML

Add to ACS ChemWorx

Figure 1 of 19

☐ **Based on DNA Strand Displacement and Functionalized Magnetic Nanoparticles: A Promising Strategy for Enzyme Immobilization**
Jiayi Song, Ping Su, Ruian Ma, Ye Yang, and Yi Yang
pp 5127-5137
Publication Date (Web): April 17, 2017 (Article)
DOI: 10.1021/acs.iecr.7b00595

Abstract | Supporting Info
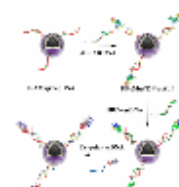
ACS ActiveView PDF
Hi-Res Print, Annotate, Reference QuickView

PDF[4187K]

PDF w/ Links[623K]

Full Text HTML

Add to ACS ChemWorx

# Calculation of the Solubility Parameter by COSMO-RS Methods and Its Influence on Asphaltene–Ionic Liquid Interactions

R. Hernández-Bravo,*,[†] A. D. Miranda,[†] O. Martínez-Mora,[‡] Z. Domínguez,[‡] J. M. Martínez-Magadán,[†] R. García-Chávez,[†] and J. M. Domínguez-Esquivel*,[†]

[†]Eje Central Lázaro Cárdenas Norte 152, Col. San Bartolo Atepehuacan, Instituto Mexicano del Petróleo, Gustavo A. Madero 07730, C. P. México

[‡]Unidad de Servicios de Apoyo en Resolución Analitica, Universidad Veracruzana, A.P. 575, Xalapa, Ver., México

Ⓢ *Supporting Information*

ABSTRACT: A study was made to determine the solubility behavior of 17 ionic liquids (ILs) with asphaltenes and a quantum-chemical density functional theory approximation using a def-TVZP basis set and the Perdew–Burke–Ernzerhof functional. The conductor-like model from COSMO-RS was used within the real solvent approximation to determine the density, molar volume, viscosity, and heat capacity with a statistical thermodynamic treatment of the interacting surface charges of the individual molecules. The solubility parameter of ILs and asphaltenes was determined using the relationship of the density and solubility parameters proposed by Panuganti et al. (*Ind. Eng. Chem. Res.* **2013**, *52*, 8009−8020). The results of the thermodynamic and solubility parameters were compared with the experimental data, and a close agreement was verified. The relative solubility of the asphaltenes with respect to ILs was determined using the δ values and Hansen's method, i.e., spheres approximation. The structure and size of the cation (including the cationic ring head and the alkyl chain length) of ILs have an influence on their ability for dispersing asphaltenes according to the molecular interactions that govern the miscibility behavior of ILs and asphaltenes, i.e., van der Waals, $\pi-\pi$, cation−π, and hydrophobic interactions.
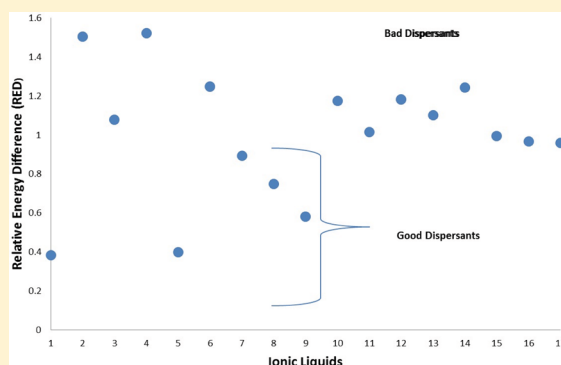
1. INTRODUCTION

Ionic liquids (ILs) are known as "green solvents", which is a consequence of their physical properties such as low vapor pressure, upper ionic conductivity, and wide electronic structure.[1,2] ILs are noncorrosive; some are reusable[3,4] and were tested successfully as catalysts for some applications.[5] Also, a molecular design of some of these systems can be made according to their specific molecular structures.[6−8]

The main applications of the ILs focused on their efficient use as "green" solvents for chemical reactions and separation processes.[9−11] In this respect, the application of computational simulations is of great interest for obtaining some thermophysical properties that are needed for engineering applications that are not always available in the open literature. Actually, it has been demonstrated that some properties such as the density and solubility parameter can be calculated using molecular dynamics for specific applications.[12,13]

In the present work, we extend the use of computational methods with the purpose of obtaining thermodynamic parameters and physicochemical data of interest such as viscosity, density, solubility parameters, molar volume, and heat capacity. Furthermore, these methods may complement the thermophysical characterization of ILs when experimental measurements are limited. In this respect, molecular simulation and modeling can contribute to calculating the thermodynamic properties and, in some cases, to predicting the behavior of particular ILs under specific conditions, which could be used in many engineering applications.

Klamt and co-workers[14,15] developed a methodology within the approximation of quantum mechanics (COSMO-RS) with the purpose of predicting the chemical potentials of fluids and solutions. COSMO-RS uses the charge density generated by quantum-mechanics calculations to describe molecules and their interactions with other molecules. The result of calculating the chemical potential of each species is to obtain thermodynamic properties. Concerning the application of COSMO-RS to the study of ILs, several publications reported the capability of this method to calculate the activity coefficients, phase equilibrium data, Hansen's solubility parameters, viscosity, density, and molar volume.[16−20]

Recent advances have been developed in COSMO-RS; for example, some relevant publications by Gonzalez-Miquel et al.[21−23] show a full analysis on the structure−property

relationship of ILs for CO_2 capture. The results show that the COSMO-RS approach can be used as a guide for designing new ILs. Also, the capture of CO_2 by ILs is related with the formation of hydrogen bonds between the cation and molecules involved.

Guo et al.[24] studied the solubility of flavonoids with respect to a large variety of ILs that were examined using COSMO-RS computations, showing a dependence of the solubility with the anion type, which helps to understand the solvation behavior for tailoring ILs as a means for esterification of flavonoids in the presence of enzymes.

Liu et al.[25] studied 357 ILs that were formed from 17 cations and 21 anions for their ability to dissolve cellulose using COSMO-RS. The logarithmic activity coefficient coincides with the experimental results. On the other hand, excess enthalpy calculations indicated that hydrogen-bonding interactions between cellulose and the seven studied ILs are key factors for the solubility of cellulose.

Boukherissa et al.[26] applied ILs as asphaltene dispersants and showed that the reduction of asphaltene aggregation occurs when ILs have good solubility in a nonpolar environment. Similarly, Firoozabadi et al.[27] studied ILs as fluid improvers for heavy petroleum crude oils. They found that a high-viscosity reduction was obtained with pyridinium ILs compared to other ILs containing different head groups. Thus, the focus of the present research was to understand better the asphaltene−IL interaction for designing newer chemical agents and for improving the flow of heavy oils by inhibiting asphaltene aggregation; this is of great technological importance[28−31] in the oil industry because of the deleterious effects caused by asphaltene precipitation, i.e., plugging of pipelines and other installations like valves, pumps, and damage in the reservoir formation.

Thus, it is of interest to design new ILs that might work as asphaltene dispersants. In this respect, the miscibility of ILs with asphaltenes might be crucial; then, we propose the use of a solubility parameter, which contains useful information on the miscibility degree as reported by Hildebrand,[32] for assessing the effects of cohesive energy (E_c) by volume (molar) unit, i.e., delta. In this respect, we propose that the potential IL− asphaltene interactions might be like surfactant (IL)− asphaltene interactions and could be assessed by δ. Additionally, the present work intends to contribute to the establishment of some principles for the molecular design of ILs and to fill the gap of thermodynamic data that have not been reported or that are very difficult to synthesize or characterize experimentally.

2. THEORETICAL CALCULATIONS

All of the geometry optimizations of the molecular structures were performed with the use of *Turbomole* software,[33] with the generalized gradient approximation Perdew−Burke−Ernzerhof functional,[34] and DFT-D3BJ damping correction methods for dispersion energy:[35] spin-polarized, automatic multiplicity, electric charge equal to zero, and a triple-valence-polarized atomic basis set (def-TZVP). The COSMO-RS files were computed using *Turbomole*. Then, the analysis for determining the thermodynamic properties was performed by COSMO-RS.[36] The COSMO-RS applications imply that all pure compounds are immersed in a perfect conductor ($\epsilon \to \infty$).

The *COSMOtherm* software calculates the pure compound liquid density ρ_i of a pure compound i from the corrected molar liquid volume V_m according to

$$\rho_i = \frac{MW_i}{V_m N_A} \tag{1}$$

MW is the molecular weight, and N_A is Avogadro's number. The corrected molar liquid volume V_m is computed from a quantitative structure−property relationship (QSPR); this methodology includes several QSPR generic parameters.

On the basis of the density values and using the correlated equation (2), one obtains the solubility parameter of ILs[37]

$$\delta = 17.347\rho + 2.904 \tag{2}$$

where ρ is the density (g/cm³). This equation is valid mainly for the liquid state,[38] in accordance with Barton[39] and Hildebrand.[32] Although eq 2 was originally proposed for nonpolar systems, the same authors applied this equation to the asphaltenes, which have a nonzero dipolar moment. Also, this equation was applied by Rogel et al.[38] for asphaltenes, using a simple relationship between the solid and liquid densities at the triple point, i.e., $\rho_s/\rho_l = 1.17$. On the basis of their phase behavior, other authors consider that asphaltenes can be treated as "nonpolar" and then only London-type van der Waals (vdW) forces apply.

Finally, the solubilities and thermodynamic properties were evaluated.

For statistical analysis, the absolute percentage error (E %) was defined as

$$E\ \% = \frac{|Valor_t - Valor_{exp}|}{Valor_{exp}} \times 100 \tag{3}$$

The ILs used in this work for the calculation are shown in Figures 1−4, while asphaltene models are illustrated in Figure 5.
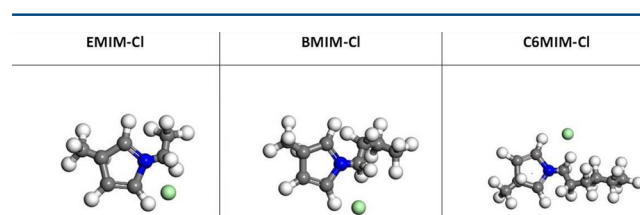

Figure 1. Molecular models of commercial ILs.[12] Atom key: gray, C; white, H; blue, N; green, Cl.
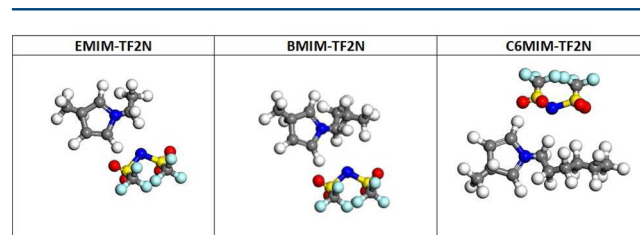
Figure 2. Molecular models of commercial ILs.[12] Atom key: gray, C; white, H; blue, N; green, Cl; red, O; yellow, S; brown, Br.

[EMIM][Cl], [BMIM][Cl], [C6MIM][Cl], [EMIM]-[TF2N], [BMIM][TF2N], [C6MIM][TF2N], and [M2][Br] were commercial samples, whereas the rest of the ILs (M1−M5 and 1A−6A) were synthesized in our research group using the methodologies described in the Supporting Information.

A total of 11 imidazole-based ILs (M1−M5 and 1A−6A), which had different alkyl tail lengths or hydroxyl or benzylic substituents at the cation as well as anions with different charge
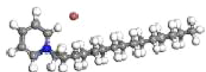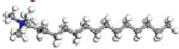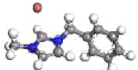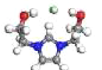
Figure 3. Nomenclature of the ILs M1−M5. Atom key: gray, C; white, H; blue, N; green, Cl; red, O; yellow, S; brown, Br.
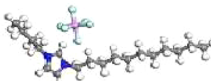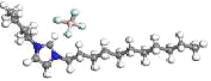
Figure 4. Nomenclature of the ILs 1A−6A. Atom key: gray, C; white, H; blue, N; green, Cl; yellow, S.

densities (chloride, bromide, hexafluorophosphate, and tetrafluoroborate), were evaluated in this work. With the purpose of testing our hypothesis, these functionalized ILs were chosen by taking into account that they could interact with asphaltenes through cation−π, π−π, hydrogen-bonding, or vdW interactions.

3. RESULTS AND DISCUSSION

The thermal stability of ILs was determined in the past by means of the strength of the formed heteroatom−hydrogen bonds and the stability of the ion species;[41] thus, the thermodynamic properties and molecular structure are key factors for designing new ILs. Then, the physical properties such as density, heat capacity, solubility, viscosity, etc., are
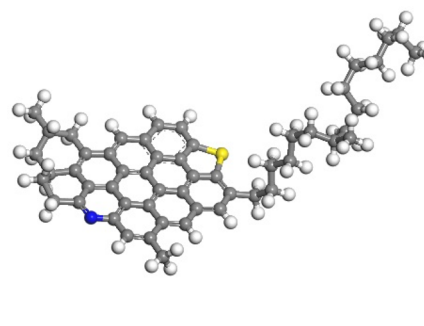
Figure 5. Asphaltene model.[40] Atom key: gray, C; white, H; blue, N; yellow, S.

important parameters in many engineering applications such as selective extraction, homogeneous phase catalysis, selective reactions, liquid membranes, etc., and their use as new materials in general.[41]

3.1. Thermodynamic Parameters. In order to demonstrate the capabilities of the COSMO-RS method to predict the thermodynamic properties, 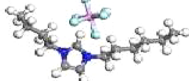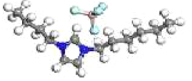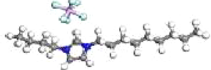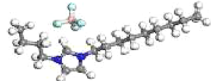some parameters of common organic solvents were calculated at 298 K for a series of known liquids and water. The results are collected in Tables 1 and 2, where the correspondence between the experimental and COSMO-RS predictions is verified by a deviation between the experimental and calculated values of ρ of less than 2.0% for heptane, toluene, and water, while it is equal or less than 3.00% for octane and benzene.

After this validation, the following step was to evaluate the density of pure ILs. All the density values in this work are collected in Table 1 in place of the Supporting Information, together with the available experimental data. The density predictions for ILs are compared in Figure 6, where the calculated density has a near-linear relationship with respect to the experimental values. The linear regression presents a correlation coefficient $R = 0.748$, which reflects the deviation from five ILs in particular, i.e., M2, M4, and 4A−6A, mainly, over 17 ILs; i.e., the percentage deviation falls between 10.5% and 16.3% for those ILs.

The trend indicates that the alkyl chain lengths of ILs seem related to lower densities, as shown in Figure 7. For alkyl side chains C_2−C_6, the nonpolar domains depend on the hydrocarbon-type chain,[42] whereas for longer alkyl side chains (C_{15} and C_{16}), the hydrophobic and electrostatic interactions are almost comparable,[43] thus contributing more to network formation and to a lower density.

Thus, the density of these nonpolar domains depends on the chain length, which is consistent with the character of the aliphatic chain with typical smaller densities. Thus, the density for these regions should be more sensitive to changes in the molecular structure of the ILs. Other physical properties such as the viscosity (see Table 2 in the Supporting Information) seem to correlate with the molecular structure of these ILs.[42,43] For example, in the systematic series [EMIM][Cl], [BMIM]-[Cl], [C6MIM][Cl], [EMIM][TF2N], [BMIM][TF2N], and [C6MIM][TF2N], this trend is verified for the same counterion, i.e., Cl or TF2N. Also, for the series 1A−6A, one verifies the same trend for hexafluorophosphate (1A, 3A, and 5A) and hexafluoroborate (2A, 4A, and 6A) counterions. Finally, for the series M1−M5, the correlation between the chain length and viscosity is less apparent; only M1−M3 show a similar viscosity for a similar chain length, while M4 and M5

Table 1. Thermodynamic Parameters of Known Organic Molecules As Obtained with COSMO-RS

model	ρ_{cal} (g/cm^3)	V_m(cal) (cm^3/mol)	viscosity$_{cal}$ (cP)	ρ_{exp} (g/cm^3)[a]	V_m(exp) (cm^3/mol)	viscosity$_{exp}$ (cP)[a]
octane	0.69	164.95	0.53	0.70	162.48	0.54
benzene	0.86	90.53	0.58	0.88	88.91	0.65
heptane	0.67	148.79	0.41	0.68	147.40	0.41
toluene	0.86	106.67	0.71	0.87	106.80	0.59
water	0.99	18.06	1.01	0.99	18.02	1.00

[a]The experimental values of known organic molecules were taken from the following: Organic Chemistry. *CRC Handbook of Chemistry and Physics*; McMurry, J., Ed.; CRC Press: Boca Raton, FL, 2006.

Table 2. Absolute Percentage Error of Known Organic Molecules[a]

	E %		
model	ρ	viscosity	V_m
octane	1.42	1.85	1.52
benzene	2.27	10.76	1.82
heptane	1.47	0.00	0.94
toluene	1.15	20.30	0.12
water	0.00	1.00	0.22

[a]The densities and heats of vaporization of the ILs M1–M5 and 1A–6A were evaluated using an Anton Paar DMA 5000 M densimeter and SDT Q600 simultaneous thermal analyzer, respectively, while the other ILs (EMIM, BMIM, and C6MIM) were reported in the literature by Derecskei and Derecskei-Kovacs.[12]
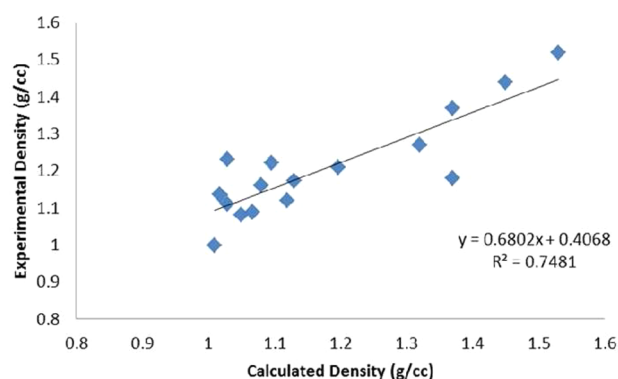

Figure 6. Comparison of the experimental and calculated COSMO-RS values of the densities of ILs.
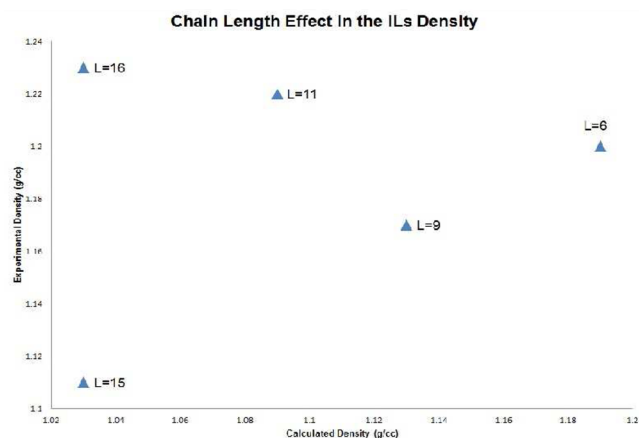
Figure 7. Chain-length effect on the density of ILs.

have the lowest viscosity and a "tail-less" structure, which should favor electrostatic interactions.

The thermodynamic parameters of ILs are shown in Table 2 in the Supporting Information. These results are important for understanding the behavior of ILs. There are several important points that stand out in this table. First, ILs have high heat capacities (C_p), which could serve for their effective application as heat accumulators, heat carriers, and reaction media in comparison with the heat capacities of materials such as iron (449 J/mol·K), magnesium (874 J/mol·K), copper (385 J/mol·K), etc.; however, other parameters are important as well, i.e., the thermal stability, heat conductivity, and viscosity. Second, ILs may have high viscosities. The viscosity is essentially dependent on intermolecular interactions (hydrogen-bonding, dispersive, and Coulombic interactions). If the vdW interactions are reduced, lower viscosities result, and this may be achieved by reducing the molecular surface area.[44] The lowest viscosities are obtained for ILs containing the EMIM ion, which contains a combination of short side chains with high mobility and low molar mass. The fluorinated alkyl chains or ILs having longer chains (1A–6A and M1–M3, respectively) result in higher viscosities because of the existence of very strong predominace of vdW interactions.[45,46] Finally, the values of the heat capacities increase with the alkyl chain length for those cases where the anion is a halogen, for example, [EMIM][Cl], [BMIM][Cl], [C6MIM][Cl], M5, and M4, but it decreases when the anion is TF2N, an alkyl chain (1A–6A) containing fluorine; thus, C_p depends not only on the cation alkyl chain length but also on the anion type.

On the other hand, the molar volumes shown in Table 2 in the Supporting Information and Figures 8 and 2 have a very good correlation with the experimental data. The linear regression fit presents an excellent correlation coefficient, i.e., $R = 0.949$. Also, the highest values of the molar volume are not associated with bulky anions (Figure 9). One observes in this figure a variation of the molar volume of an IL with the same

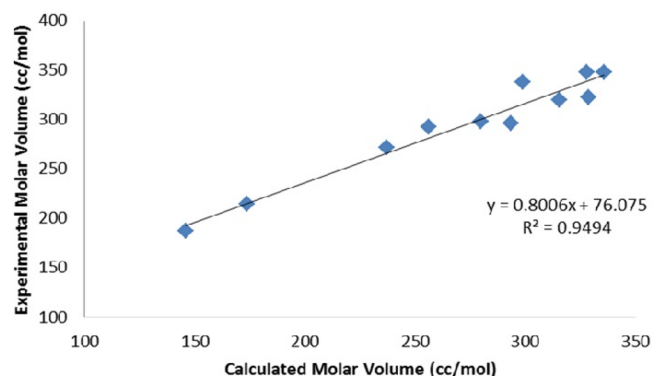**Figure 8.** Comparison of the experimental and calculated COSMO-RS values of the molar volume.
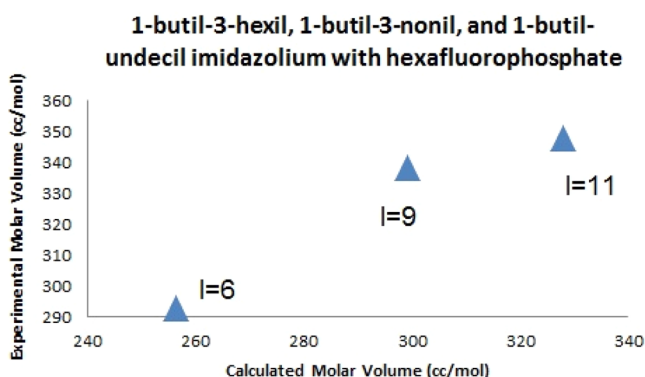
Figure 9. Chain-length effect of the ILs on the molar volume.

imidazolium cation and hexafluorophosphate anion but different lengths of the alkyl chain; thus, the molar volume increases.

The experimental molar volume is calculated using the equation proposed by Chotaray:

$$V_m = \frac{M}{N_A \rho} \tag{4}$$

where M is the molecular weight of the ILs, N_A is Avogrado's number (6.022×10^{23} mol^{-1}), and ρ is the experimental density value.

Therefore, as discussed above for the case of the density, there is a strong influence of the side (alkyl) chain because the polar and nonpolar domains seem to affect considerably the thermodynamic properties.

3.2. Solubility Parameters of ILs. The values of the solubility parameters of [EMIM][Cl], [BMIM][Cl], and [C6MIM][Cl] were estimated from the experimental density values using the empirical equation (2) and are reported in Table 3. The values of the solubility parameters for the asphaltenes are computational calculations; the first column reports the values using NPT molecular dynamics,[47] while the second column reports the values that were obtained with the equations used in this work.

Table 3. Values of the Solubility Parameters of ILs and Asphaltenes

model	δ(exp) (MPa$^{0.5}$)	δ(cal) (MPa$^{0.5}$)	E %
[EMIM][Cl]	22.3	22.3	0.0
[EMIM][TF2N]	27.6	29.5	6.8
[BMIM][Cl]	21.6	21.1	2.3
[BMIM][TF2N]	26.7	27.9	4.5
[C6MIM][Cl]	20.3	20.4	0.5
[C6MIM][TF2N]	25.6	26.7	4.3
M1	19.2	20.8	8.3
M2	19.4	20.8	7.2
M3	19.8	21.7	9.5
M4	21.4	26.6	24.3
M5	24.2	25.8	6.6
1A	24.1	23.7	1.7
2A	21.9	21.4	2.3
3A	25.1	22.5	10.4
4A	22.8	20.6	9.7
5A	24.6	21.9	10.9
6A	22.8	20.2	11.4
asphaltene	19.5	20.2	3.6

Recently, Rogel et al.[38] reported that the solubility parameters from eq 2 were too high compared with the reported values of polyaromatics, for example, hexabenzocoronene (21−22 MPa$^{0.5}$),[48] graphene (21−22 MPa$^{0.5}$),[49] single-walled nanotubes (21 MPa$^{0.5}$),[50] and C$_{60}$ (19.5 MPa$^{0.5}$).[51] Thus, these authors used a simple equation for relating the solid and liquid densities at the triple point[52] as follows:

$$\frac{\rho_s}{\rho_1} = 1.17 \tag{5}$$

This ratio has been found to be adequate and reliable in determining the solubility parameters of the asphaltenes.[38]

Table 3 shows the results that were obtained using the model represented in Figure 5 and eq 2. As observed, there is an agreement of the experimental values with the theoretical values reported in the literature for the series [EMIM][TF2N], [BMIM][TF2N], and [C6MIM][TF2N] as well as for the experimental series M1−M5 and 1A−6A. The values obtained for commercial ILs correlate very well with those obtained in our calculations, with a percentage error of less than 10%, which is considered acceptable for the complex organic molecules. In the case of ILs that were developed in the present work, the percentage error is less than 10%, except for the IL M4, which shows a rather large error; however, this is not indicative of a failure of the present methodology because there is an agreement for the other cases.

The solubility parameters decrease progressively with an increase of the side-chain length, which is consistent with a more aliphatic character. These results are shown in Figure 10.
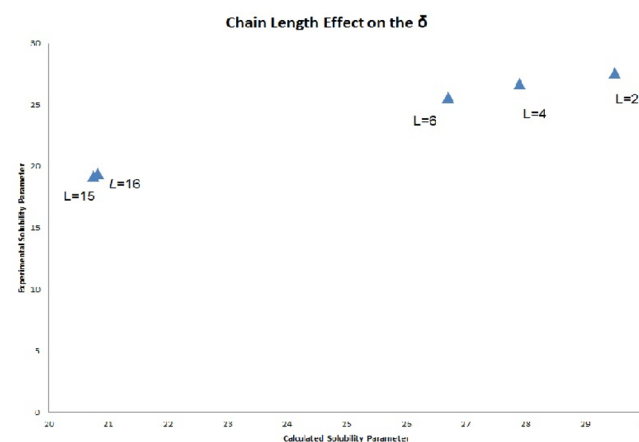
Figure 10. Alkyl chain-length effect on the solubility parameter of ILs.

ILs with long alkyl chains tend to decrease the solubility parameters; i.e., they are closer to the solubility parameters of the asphaltenes, as described by Barton: "materials with similar values of solubility parameters are likely to be miscible".[32,39] ILs that present a better behavior as asphaltene dispersants are M1−M3, 4A, and 6A.

On the basis of this analysis, the solubility parameter of the asphaltene is shown in Table 3.

The asphaltene solubility parameter is in a range between 19.5 and 20.2, which means, according to Hildebrand,[32] that ILs can behave as asphaltene dispersants because their values are close.

However, the IL structure affects the Hildebrand solubility parameter.[32] ILs having different types of anions and cations may have different polarities, which induces different molecular

interaction forces. Therefore, we estimated two solubility parameters for ILs: δ_{NP} for nonpolar families and δ_p for polar families. This is due to the amphiphilic behavior of ILs. In order to strengthen the discussion, we determined Hansen's solubility parameters.[53]

Hansen's extension of the solubility parameter to a 3D system was based on the hypothesis that the cohesive energy depends on the sum of nonpolar, polar, and hydrogen-bonding molecular interactions. Thus, the solubility parameter splits into a dispersion force component (δ_d), a hydrogen-bonding component (δ_h), and a polar component (δ_p), which are additive. Thus, for each molecule, there are three Hansen parameters:[53]

$$\delta_t{}^2 = \delta_d{}^2 + \delta_p{}^2 + \delta_h{}^2 \qquad (6)$$

where δ_d is the energy from dispersion forces, δ_p is the energy from dipolar intermolecular forces, and δ_h is the energy from hydrogen-bonding forces. In this work, only the dispersive and electrostatic terms of the solubility parameters are considered.

Dispersion forces are the weakest type of noncovalent interactions, which are within the so-called supramolecular interactions. The formation of supramolecular complexes through interactions of the ionic-pair type is the most stable. In relation to ILs and asphaltenes, the forces that govern the miscibility are cation−π interactions. The presence of cation−π interactions favorably affects the solubility of aromatic compounds in ILs,[54] and it affects the enthalpy and entropy of the IL structure.[55]

In order to calculate the contribution of permanent dipoles to the cohesive energy density, the formula proposed by Beerbower was used.[56] The dipole moment and molar volume values were obtained from the *Turbomole* and COSMO-RS calculations, respectively (see eq 7).

$$\delta_p = 9.5 \frac{\mu}{V_m{}^{1/2}} \qquad (7)$$

From eq 8, the dispersive contribution was obtained:

$$\delta_d{}^2 = \delta_t{}^2 - \delta_p{}^2 \qquad (8)$$

The results of the dipole moments and dispersive and electrostatic terms to the solubility parameters are shown in Table S3 in the Supporting Information. The values of the electrostatic terms of the ILs are above the asphaltene value; this indicates that the solubility of asphaltenes in ILs depends exclusively on the dispersive contribution.

Finally, the calculated δ values were used for a further calculation of the solubility of asphaltenes in ILs using Scatchard−Hildebrand's theory,[57] where the relative solubility, ΔS_R, is calculated as follows (eq 9):

$$\Delta S_R = \exp\left[-\frac{V_{asphal}}{RT}(\delta_{solv} - \delta_{asphal})^2\right] \qquad (9)$$

where V_{asphal}, δ_{solv}, and δ_{asphal} are the molar volume and solubility parameters of solvents and asphaltenes, respectively. The maximum of the solubility occurs when the cohesive energy densities are identical ($\delta_{solv} = \delta_{asphal}$ and $\Delta S_R = 1$). This method provides a solubility prediction; however, some mistakes might occur; for example, a good solvent may have the same δ value compared with a bad solvent. Alternatively, the methods developed by Hansen[53] seem more interesting for exploring the asphaltene solubility.

In this case, the solubility is described by a spherical solubility region centered at the asphaltene system. The boundaries of the solubility region are given by the radius R_A:[47]

$$R_A = \sqrt{4(\delta_d{}^{asph} - \delta_d{}^{solv})^2 + (\delta_p{}^{asph} - \delta_p{}^{solv})^2 + (\delta_h{}^{asph} - \delta_h{}^{solv})^2} \qquad (10)$$

δ_d, δ_p, and δ_h are the dispersive, electrostatic, and hydrogen-bonding components of δ. In the present case, only the dispersive and electrostatic components were used as reported in Table 3 in the Supporting Information. Thus, the relative energy difference (RED) corresponds to the distance R_A of the solubility parameter of the solvent from the center of the sphere divided by R_0, which is the radius of the sphere:[47]

$$RED = \frac{R_A}{R_0} \qquad (11)$$

R_A is calculated from eq 10. For good solvents, RED $\leq$ 1, while bad solvents show values of RED $\geq$ 1.[47] The highest solubility corresponds to RED = 0.

The calculated RED values for the asphaltene model in ILs are reported in Table 4. In the present work, the trend of the solubility in ILs, as suggested by RED, is [EMIM][Cl] $\geq$ [C6MIM][Cl] $\geq$ M3 $\geq$ M2 $\geq$ M1 $\geq$ 6A $\geq$ 5A $\geq$ 4A $\geq$ M5 $\geq$ [BMIM][Cl].

Table 4. Relative Solubilities of Asphaltene Models in ILs

model	RED	model	RED	model	RED
[EMIM][Cl]	0.385	M1	0.893	1A	1.183
[EMIM][TF2N]	1.504	M2	0.749	2A	1.102
[BMIM][Cl]	1.079	M3	0.581	3A	1.244
[BMIM][TF2N]	1.521	M4	1.174	4A	0.995
[C6MIM][Cl]	0.399	M5	1.014	5A	0.966
[C6MIM][TF2N]	1.247			6A	0.960

It is clear that the structure and size of the cation (i.e., including the cationic head ring and the alkyl chain length) of an IL have a significant effect on the solvent ability for dispersing asphaltenes, as shown in Table 4. An increase of the alkyl chain length of the cation can dramatically increase the asphaltene solubility in ILs except for [EMIM][Cl]. The solubility of [EMIM][Cl] may be related with other interactions that are present and promote the asphaltene stability in ILs, for example, π−π interaction (π−π stacking) between the asphaltene and 1-ethyl-3-methylimidazolium chloride. Some ILs that present bulky anions (TF2N and 1A−3A) and a smaller alkyl chain tend to decrease the solubility of the ILs in the asphaltenes. The effect of the heteroatoms in ILs plays an important role also because their capacity of charge transfer, which is observed for [BMIM][Cl], where there is a considerable increase in the electrostatic contribution compared with [EMIM][Cl] and [C6MIM][Cl] (see Table 3 in the Supporting Information). On the other hand, ILs with large alkyl chain lengths (M1−M3, 5A, and 6A) show that hydrophobic interactions predominate because the amphiphilic character of the ILs, which dominate the miscibility behavior of both ILs and asphaltenes; however, the cation−π interactions are attractive between the cationic head of the ILs and the cloud π of the asphaltenes.

Therefore, the molecular structure of the ILs must be oriented according to the molecular interactions that predominate in the asphaltenes; then stabilization can occur.

In summary, the dispersion ability of amphiphiles has been extensively discussed in the literature in terms of the stabilization energy, that is, the interaction energy of asphaltenes with dispersant agents.[26] The capacity of an amphiphile as an asphaltene stabilizer depends mainly on its chemical and structural characteristics.[58] In this way, ILs having a polar head and an alkyl chain may have surfactant characteristics. On the other hand, it is widely known in the literature that the activity of the amphiphiles as asphaltene dispersants depends on the strength of the asphaltene–amphiphile interactions,[59] in this respect, the solubility parameter indicates the cohesive energy by the volume unit (eq 12) according to Hildebrand[32] for those molecules, i.e.

$$\delta = \sqrt{\frac{E_{\text{cohesive}}}{V_{\text{m}}}} \tag{12}$$

Thus, this work verifies the relationship of the solubility parameter with the asphaltene dispersion properties of ILs. Finally, the molecular structure of the asphaltene dispersants consists of two parts, a polar group (due to the presence of heteroatoms like oxygen, nitrogen, and phosphorus), which attaches to the asphaltene core, and an alkyl group, which prevents the formation of nanoaggregates.[60] These two groups are able to interact only if a long alkyl tail exists because they should have the ability to change the polarity of the surface of the aggregates and should prevent the precipitation of asphaltenic aggregates.[61,62]

4. CONCLUSIONS

The synthesis of some ILs and their physical properties were systematically analyzed in the framework of the COSMO-RS approach, for calculating their thermodynamic properties, i.e., density, viscosity, heat capacity, molar volume, etc. The densities, molar volumes, and solubility parameters of 17 ILs were in agreement with the experimental values. With this basis, the solubility of the asphaltenes in ILs was explored using the calculated δ values and Hansen's sphere method. From these results, the order of the solubility was the following: [EMIM][Cl] ≥ [C6MIM][Cl] ≥ M3 ≥ M2 ≥ M1 ≥ 6A ≥ 5A ≥ 4A ≥ M5 ≥ [BMIM][Cl]. The structure and size of the IL's cation (including the cationic head ring and the alkyl chain length) have an influence on their ability to disperse asphaltenes according to the types of molecular interactions, which govern the miscibility behavior of ILs and asphaltenes by vdW, π–π, cation–π, and hydrophobic interactions.

■ ASSOCIATED CONTENT

ⓢ Supporting Information

The Supporting Information is available free of charge on the ACS Publications website at DOI: 10.1021/acs.iecr.6b05035.

> Synthesis and spectroscopic characterization of ILs, density and thermodynamic parameters of ILs (Tables 1 and 2), and dipole moments and solubility parameter contributions of ILs (Table 3) (PDF)

■ AUTHOR INFORMATION

Corresponding Authors
*E-mail: raizahernandezbravo@gmail.com (R.H.-B.).

*E-mail: jmdoming@imp.mx (J.M.D.-E.).

ORCID ⓘ
R. Hernández-Bravo: 0000-0002-6608-8135

Notes
The authors declare no competing financial interest.

■ ACKNOWLEDGMENTS

■ REFERENCES

(1) Gardas, R.; Freire, M.; Carvalho, P.; Marrucho, I.; Fonseca, I.; Ferreira, A.; Coutinho, J. PρT Measurements of Imidazolium-Based Ionic Liquids. *J. Chem. Eng. Data* **2007**, *52*, 80–88.

(2) Holbrey, J. D.; Seddon, K. R. Ionic Liquids. *Clean Technol. Environ. Policy* **1999**, *1*, 223–236.

(3) Earle, M. J.; Seddon, K. R. Ionic Liquids.Green Solvents for the Future. *Pure Appl. Chem.* **2000**, *72*, 1391–1398.

(4) García-Bernal, E.; de los Rios, A.; Hernández-Fernández, F.; Larrosa-Guerrero, A.; Ginestá, A.; Sánchez-Segado, S.; Lozano, L.; Godínez, C. Aplicaciones de los líquidos Iónicos en la Industria Química. *Jornadas a la Investigación de la UPCT* **2011**, 66–68.

(5) Katritzky, A. R.; Jain, R.; Lomaka, A.; Petrukhin, R.; Karelson, M.; Visser, A. E.; Rogers, R. Correlation of the Melting Points of Potential Ionic Liquids (Imidazolium Bromides and Benzimidazolium Bromides) Using the CODESSA Program. *J. Chem. Inf. Comput. Sci.* **2002**, *42*, 225–231.

(6) Derecskei, B.; Derecskei-Kovacs, A. Molecular Dynamics Studies of the Compatibility of Some Cellulose Derivates with Selected Ionic Liquids. *Mol. Simul.* **2006**, *32*, 109–115.

(7) Hanke, C. G.; Price, S. L.; Lynden-Bell, R. M. Intermolecular Potentials for Simulations of Liquid Imidazolium Salts. *Mol. Phys.* **2001**, *99*, 801–809.

(8) de Andrade, J.; Böes, E. S.; Stassen, H. A Force Field for Liquid State Simulations on Room Temperature Molten Salts: 1-Ethyl-3-methylimidazolium Tetrachloroaluminate. *J. Phys. Chem. B* **2002**, *106*, 3546–3548.

(9) Martínez-Magadán, J. M.; Oviedo-Roa, R.; García, P.; Martínez-Palou, R. DFT Study of the Interaction between Ethanethiol and Fe-containing Ionic Liquids for Desulfuration of Natural Gasoline. *Fuel Process. Technol.* **2012**, *97*, 24–29.

(10) Velarde, M.; Gallo, M.; Alonso, P. A.; Miranda, A. D.; Domínguez, J. M. DFT Study of the Energetic and Noncovalent Interactions between Imidazolium Ionic Liquids and Hydrofluoric Acid. *J. Phys. Chem. B* **2015**, *119*, 5002–5009.

(11) Li, H.; Chang, Y.; Zhu, W.; Jiang, W.; Zhang, M.; Xia, J.; Yin, S.; Li, H. A DFT Study of the Extractive Desulfurization Mechanism by [BMIM])+[AlCl4]− Ionic Liquid. *J. Phys. Chem. B* **2015**, *119*, 5995–6009.

(12) Derecskei, B.; Derecskei-Kovacs, A. Molecular Modelling Simulations to Predict Density and Solubility Parameters of Ionic Liquids. *Mol. Simul.* **2008**, *34*, 1167–1175.

(13) Del Pópolo, M.; Lynden-Bell, R. M.; Kohanoff, J. Ab Initio Molecular Dynamics Simulation of a Room Temperature Ionic Liquid. *J. Phys. Chem. B* **2005**, *109*, 5895–5902.

(14) Klamt, A.; Schuurmann, G. COSMO: A New Approach to Dielectric Screening in Solvents with Explicit Expresions for the Screening energy and its gradient. *J. Chem. Soc., Perkin Trans. 2* **1993**, 799–805.

(15) Klamt, A. Conductor-like Screening Model for Real Solvents: A New Approach to the Quantitative Calculation of Solvation Phenomena. *J. Phys. Chem.* **1995**, *99*, 2224–2235.

(16) Ferreira, A. R.; Freire, M. G.; Ribeiro, J. C.; Lopes, F. M.; Crespo, J. G.; Coutinho, J. Ionic Liquids for Thiols Desulfurization: Experimental Liquid-Liquid Equilibrium and COSMO-RS Description. *Fuel* **2014**, *128*, 314−329.

(17) Grabda, M.; Panigrahi, M.; Oleszek, S.; Kozak, D.; Eckert, F.; Shibata, E.; Nakamura, T. COSMO-RS Screening for Efficient Ionic Liquid Extraction Solvents for NdCl$_3$ and DyCl$_3$. *Fluid Phase Equilib.* **2014**, *383*, 134−143.

(18) Járvás, G.; Quellet, C.; Dallos, A. Estimation of Hansen Solubility Parameters Using Multivariate Nonlinear QSPR Modeling with COSMO Screening Charge Density Moments. *Fluid Phase Equilib.* **2011**, *309*, 8−14.

(19) Zhao, Y.; Huang, Y.; Zhang, X.; Zhang, S. A Quantitative Prediction of the Viscosity of Ionic Liquids Using $S_{\sigma-profile}$ Molecular Descriptor. *Phys. Chem. Chem. Phys.* **2015**, *17*, 3761−3767.

(20) Palomar, J.; Ferro, V.; Torrecilla, J. S.; Rodríguez, F. Density and Molar Volume Predictions Using COSMO-RS for Ionic Liquids. An Approach to Solvent Design. *Ind. Eng. Chem. Res.* **2007**, *46*, 6041−6048.

(21) González-Miquel, M.; Talreja, M.; Ethier, A. L.; Flack, J. R.; Switzer, E.; Biddinger, P.; Pollet, P.; Palomar, J.; Rodríguez, F.; Eckert, C.; Liotta, C. COSMO-RS Studies: Structures-Properly Relationsships for CO_2 Capture by Reversible Ionic Liquids. *Ind. Eng. Chem. Res.* **2012**, *51*, 16066−16073.

(22) González-Miquel, M.; Palomar, J.; Rodríguez, F. Selection of Ionic Liquids for Enhancing the Gas Solubility of Volatile Organic Compounds. *J. Phys. Chem. B* **2013**, *117*, 296−306.

(23) González-Miquel, M.; Massel, M.; Desilva, A.; Palomar, J.; Rodríguez, F.; Brennecke, J. Excess Enthalpy of Monoethanolamine. Ionic Liquids Mixtures: How Good are COSMO-RS Predictions? *J. Phys. Chem. B* **2014**, *118*, 11512−11522.

(24) Guo, Z.; Lue, B.; Thomasen, K.; Meyer, A.; Xu, X. Predictions of Flavonoids Solubility in Ionic Liquids by COSMO-RS: Experimental, Verification, Structural Elucidation, and Solvation Characterization. *Green Chem.* **2007**, *9*, 1362−1373.

(25) Liu, Y.; Thomsen, K.; Nie, Y.; Zhang, S.; Meyer, A. Predictive Screening of Ionic Liquids for Dissolving Cellulose and Experimental Verification. *Green Chem.* **2016**, *18*, 6246−6254.

(26) Boukherissa, M.; Mutelet, F.; Modarressi, A.; Dicko, A.; Dafri, D.; Rogalski, M. Ionic Liquids as Dispersants of Petroleum Asphaltenes. *Energy Fuels* **2009**, *23*, 2557−2564.

(27) Subramanian, D.; Wu, K.; Firoozabadi, A. Ionic Liquids as Viscosity Modifiers for Heavy and Extra-heavy Crude Oils. *Fuel* **2015**, *143*, 519−526.

(28) Rashid, Z.; Wilfred, C. D.; Murugesan, T. Asphaltene Separation with Designer Solvents for the Deasphaltenes Process-A Quantum Chemical Approach. *Procedia Eng.* **2016**, *148*, 268−274.

(29) Rezaee Nezhad, E.; Heidarizadeh, F.; Sajjadifar, S.; Abbasi, Z. Dispersing of Petroleum Asphaltenes by Acidic Ionic Liquid and Determination by UV−Visible Spectroscopy. *J. Pet. Eng.* **2013**, *2013*, 1−5.

(30) Murillo-Hernández, J. A; Aburto, J. *Current Knowledge and Potential Applications of Ionic Liquids in the Petroleum Industry,Ionic Liquids: Applications and Perpectives*; InTech, 2011.

(31) Murillo-Hernández, J. A.; García-Cruz, I.; López-Ramírez, S.; Duran-Valencia, C.; Domínguez, J. M.; Aburto, J. Aggregation Behavior of Heavy-Crude Oil-Ionic Liquids Solutions by Fluorescence Spectroscopy. *Energy Fuels* **2009**, *23*, 4584−4592.

(32) Hildebrand, J. H. *The Solubility of Non-Electrolytes*; Reinhold: New York, 1936.

(33) *Tmolex*, version 4.0; Cosmologic GmbH & Co. KG: Alemania.

(34) Perdew, J. P.; Burke, K.; Ernzerhof, M. Generalized Gradient Approximation. *Phys. Rev. Lett.* **1996**, *77*, 3865−3868.

(35) Grimme, S.; Ehrlich, S.; Goerigk, L. Effect of the Damping Function in Dispersion Corrected Density Functional Theory. *J. Comput. Chem.* **2011**, *32*, 1456−1465.

(36) Echert, F.; Klamt, A. *COSMOtherm*, version C301401, release 0111; Cosmologic GmbH & Co. KG, 1999.

(37) Panuganti, S.; Vargas, F.; Chapman, W. Property Scaling Relations for Nonpolar Hydrocarbons. *Ind. Eng. Chem. Res.* **2013**, *52*, 8009−8020.

(38) Rogel, E.; Miao, T.; Vien, J.; Roye, M. Comparing Asphaltenes: Deposit versus Crude Oil. *Fuel* **2015**, *147*, 155−160.

(39) Barton, A. F. M. *Handbook of solubility parameters and other cohesion parameters*, 2nd ed.; CRC Press: Boca Raton, FL, 1991.

(40) Zajac, T.; Sethi, N. K.; Joseph, J. T. Molecular Imaging of Petroleum Asphaltenes by Scanning Tunneling Microscopy. *Scanning Microscopy.* **1994**, *8*, 463−470.

(41) Anthony, J. L.; Brennecke, J. F.; et al. Physicochemical properties of ionic liquids. In *Ionic Liquids in Synthesis*; Wasserscheid, P., Welton, T., Eds.; Wiley-WCH: Weinheim, Germany, 2003; pp 41−126.

(42) Shimizu, K.; Costa-Gomes, M.; Pádua, A.; Rebelo, L.; Canongia-Lopes, J. Three Commentaries on the Nano-Segregated Structure of Ionic Liquids. *J. Mol. Struct.: THEOCHEM* **2010**, *946*, 70−76.

(43) Rocha, M.; Lima, C.; Gomes, L.; Schroder, B.; Coutinho, J.; Marrucho, I.; Esperanca, J.; Rebelo, L.; Shimizu, K.; Lopes, J. N. C.; Santos, L. High-Accuracy Vapor Pressure Data of the Extended $[C_nC_1im][Ntf_2]$ Ionic Liquids Series: Trend Changes and Structural Shifts. *J. Phys. Chem. B* **2011**, *115*, 10919−10926.

(44) Park, S.; Kazlauskas, R. J. Biocatalysis in Ionic Liquids-Advantages Beyond Green Technology. *Curr. Opin. Biotechnol.* **2003**, *14*, 432−437.

(45) Freire, M. G.; Teles, A. R.; Rocha, M.; Schroder, B.; Neves, C.; Carvalho, P. J.; Evtuguin, D.; Santos, L.; Coutinho, J. Thermophysical Characterization of Ionic Liquids Able To Dissolve Biomass. *J. Chem. Eng. Data* **2011**, *56*, 4813−4822.

(46) Shen, S.; Fang, S.; Qu, L.; Luo, D.; Yang, L.; Hirano, S. Low-viscosity Ether-functionalized Pyrazolium Ionic Liquids based on Dicyanamide anions: Properties and Application as Electrophyles for Lithium Metal Batteries. *RSC Adv.* **2015**, *5*, 93888−93899.

(47) Aray, Y.; Hernández-Bravo, R.; Parra, J. G.; Rodríguez, J.; Coll, D. Exploring the Structure-Solubility Relationship of Asphaltenes Models in Toluene, Heptane, and Amphiphiles Using a Molecular Dynamic Atomistic Methodology. *J. Phys. Chem. A* **2011**, *115*, 11495−11507.

(48) Hughes, J. M.; Hernández, Y.; Aherne, D.; Doessel, L.; Mullen, K.; Moreton, B.; White, T. W.; Partridge, C.; Costantini, G.; Shmeliov, A.; Shannon, M.; Nicolosi, V.; Coleman, J. N. High Quality Dispersions of Hexabenzocoronene in Organic Solvents. *J. Am. Chem. Soc.* **2012**, *134*, 12168−12179.

(49) Hernández, Y.; Lotya, M.; Rickard, D.; Bergin, S.; Coleman, J. Measurement of Multicomponent Solubility Parameters for Graphene Facilities Solvent Discovery. *Langmuir* **2010**, *26*, 3208−3213.

(50) Bergin, S.; Sun, Z.; Rickard, D.; Streich, P. V.; Hamilton, J.; Coleman, J. Multicomponent Solubility Parameters for Single-Walled Carbon Nanotubes-Solvent Mixtures. *ACS Nano* **2009**, *3*, 2340−2350.

(51) Cataldo, F. On the Solubility Parameters of C60 and Higher Fullerenes. *Fullerenes, Nanotubes, Carbon Nanostruct.* **2009**, *17*, 79−84.

(52) Goodman, B. T.; Wilding, W. V.; Oscarson, J. L.; Rowley, R. A Note on the Relationsship between Organic Solid Density and Liquid Density at the Triple Point. *J. Chem. Eng. Data* **2004**, *49*, 1512−1514.

(53) Hansen, C. M. The Three Dimensional Solubility Parameter. *J. Paint. Technol.* **1967**, *39*, 104−505.

(54) Blanchard, L. A.; Brennecke, J. F. Recovery of Organic Products from Ionic Liquids Using Supercritical Carbon Dioxide. *Ind. Eng. Chem. Res.* **2001**, *40*, 287−292.

(55) Krossing, I.; Slattery, J. M.; Daguenet, C.; Dyson, P. J.; Oleinikova, A.; Weingartner, H. Why are Ionic Liquid? A Simple Explanation Based on Lattice and Solvation Energies. *J. Am. Chem. Soc.* **2006**, *128*, 13427−13434.

(56) Beerbower, A. Surface Free Energy: A New Relationship to Bulk Energies. *J. Colloid Interface Sci.* **1971**, *35*, 126−132.

(57) Scatchard, G. Equilibria in Non-electrolyte Solutions in Relation to the Vapor Pressures and Densities of the Components. *Chem. Rev.* **1931**, *8*, 321−333.

(58) Chang, C. L.; Fogler, H. S. Stabilization of Asphaltenes in Aliphatic Solvents Using alkylbenzene-derived Amphiphiles.1. Effect of the Chemical Structure of Amphiphile on Asphaltene Stabilization. *Langmuir* **1994**, *10*, 1749−1757.

(59) Rogel, E.; Contreras, E.; León, O. An Experimental Theoretical Approach to the Activity of Amphiphiles as Asphaltenes Stabilizers. *Pet. Sci. Technol.* **2002**, *20*, 725−739.

(60) Firoozinia, H.; Fouladi Hossein Abad, K.; Varamesh, A. A Comprehensive Experimental Evaluation of Asphaltene Dispersants for Injection under Reservoir Conditions. *Pet. Sci.* **2016**, *13*, 280−291.

(61) Barcenas, M.; Orea, P.; Buenrostro-Gonzalez, E.; Zamudio-Rivera, L. S.; Duda, Y. Study of Medium Effect on Asphaltenes Agglomeration Inhibitor Efficiency. *Energy Fuels* **2008**, *22*, 1917−1922.

(62) Ferrara, M. Hydrocarbons Oil-Aqueous Fuel and Additive Compositions. WO Patent, 1995; p 637.